Upgrading the Melt Flow Index to Rheogram Approach in the Low Shear Rate Region*

A. V. SHENOY and D. R. SAINI, *Polymer Science and Engineering Group, Chemical Engineering Division, National Chemical Laboratory, Pune 411008, India*

Synopsis

The unified viscosity function curves proposed earlier by the authors have an inherent limitation in the low shear rate region. This limitation is the effect of using the melt flow index as a normalizing factor to obtain the coalesced curves, which itself is insensitive to molecular parameters such as molecular weight distribution. A single integral constitutive equation of the BKZ type is used to derive the viscosity function which would be useful in generating unified curves based on the melt flow index but devoid of the limitation of molecular weight distribution effects in the low shear rate region.

INTRODUCTION

It is well known that all polymer melts are viscoelastic, and, therefore, it is essential to understand the viscous and elastic responses of these materials to deformation during processing. It has been the general practice to study the viscous and elastic responses separately through the use of two material functions, namely, the viscosity function η and the primary normal stress function ψ_1. During processing, the polymer melt is subjected to a wide range of shear rates and varied temperatures. The variations in the viscosity and primary normal stress functions with shear rates and temperatures are to be known for process optimization and control, process design, and trouble-shooting. The necessary data on the viscosity function are collected through capillary rheometers or rotational viscometers. The normal stress difference data, however, require the use of rotational viscometers alone. In either case, the equipments needed for the generation of such data are highly sophisticated and very expensive. They are time-consuming and require trained operators. Hence, though generation of such data is essential from the point of view of the plastics processor, the measuring instruments are beyond the financial capacity and the technical abilities of most of them.

Shenoy et al.[1-5] have recently suggested simple methods for estimating the two material functions η and ψ_1 through the use of the material parameter, which is generally used for quality control, namely, the melt flow index (MFI). A number of unified curves which are grade- and temperature-invariant have been given for a wide variety of polymer grades so that a rheogram of η vs. $\dot{\gamma}$ as well as a plot of N_1 vs. $\dot{\gamma}^2$ can be estimated merely through the knowledge of the MFI, which is either provided by the polymer manufacturer or can be determined simply through the use of the relatively inexpensive melt flow indexer. The

* NCL Communication No. 3149.

Journal of Applied Polymer Science, Vol. 29, 1581–1593 (1984)
 CCC 0021-8995/84/051581-13$04.00

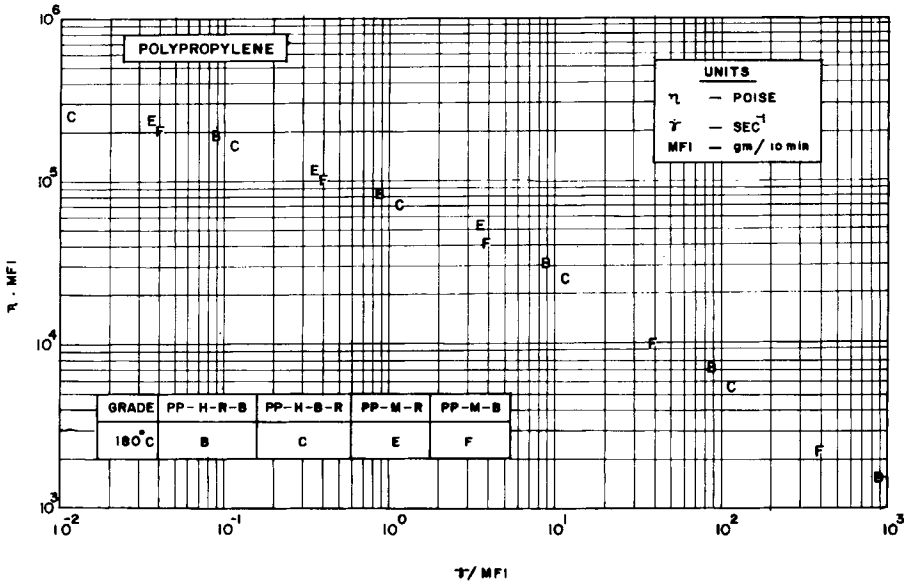

Fig. 1. Coalesced viscosity curve for broad and regular molecular weight distribution PP at 2.16-kg test load condition for MFI.

generation of the unified curves involved the coalescence of the original η vs. $\dot{\gamma}$ curves for the viscosity function by plotting η·MFI vs. $\dot{\gamma}$/MFI on a log–log scale and the coalescence of the original ψ_1 vs. $\dot{\gamma}^2$ curves for the primary normal stress function by plotting ψ_1·(MFI)^2 vs. ($\dot{\gamma}$/MFI)^2 on a log–log scale. The coalescence was governed by the shape of the original curves and similar shaped curves, undoubtedly, coalesced better. The shapes of the curves are dependent upon molecular parameters such as molecular weight distribution. The melt flow index is itself insensitive to subtle changes in molecular parameters, as has been shown by Smith,[6] Borzenski,[7] and Shida and Cancio.[8] Since MFI has been used as a normalizing factor during coalescence,[1–4] the unified curves, too, are insensitive to changes in molecular weight distribution. The effects of differences in molecular weight distribution are seen in the low shear rate and very high shear rate region. However, since the width of shear rates of interest for most polymer processing operations lie within the medium range, the unified curves[1–4] for the viscosity function are very handy tools for most processors.

The primary normal stress difference function exhibits a strong dependence on molecular weight distribution as predicted from the theory of second-order fluids.[9] Moreover, normal stress difference data is generally collected on rotational viscometers, which have an effective upper limit of shear rate not greater than 10 s^{-1}. Thus, it is essential to include the effects of molecular weight distribution in the unified normal stress difference curves if unique curves are to be obtained which are invariant for the width of the molecular weight distribution. Shenoy and Saini[5] have used plots of N_1 vs. $(\overline{M}_z/\overline{M}_w)^{3.5}$ ($\dot{\gamma}$/MFI)^2 on a log–log scale to obtain unique curves for a number of polymers of different generic type.

The purpose of the present paper is to develop a method for obtaining unique

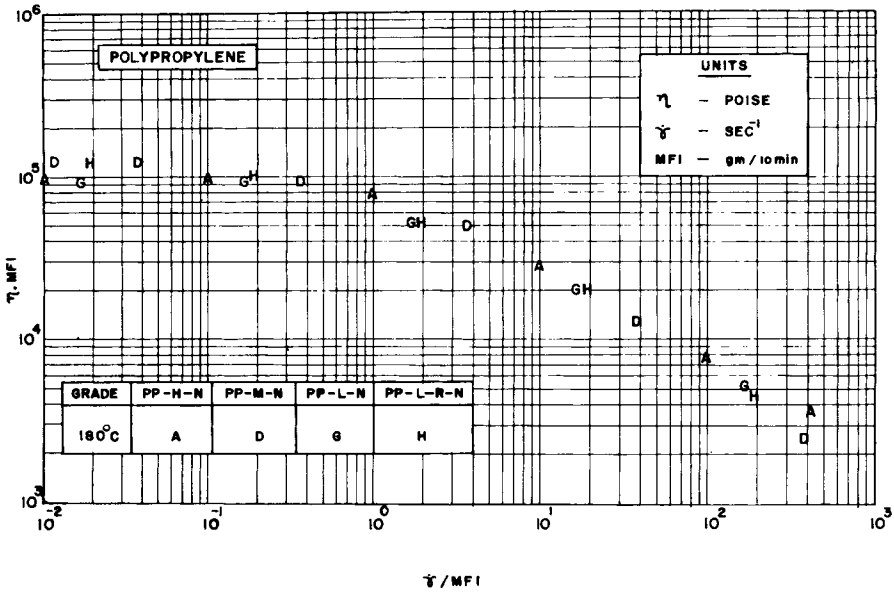

Fig. 2. Coalesced viscosity curve for four narrow molecular weight distribution PP at 2.16-kg test load condition for MFI.

curves in the low shear rate regions so that the limitation of molecular weight distribution on the unified viscosity curves of Shenoy et al.[1-4] is effaced. The propriety of the approach suggested herein is tested for three different types of polyolefins, namely, polypropylene, low density polyethylene, and high density polyethylene.

THEORETICAL ANALYSIS

Shenoy and Saini[10] have modified the relationship suggested by Wagner[11] between the primary normal stress function ψ_1 and the viscosity function η for fitting the temperature and grade-invariant unified normal stress curves[5] and the unified viscosity curves.[1-4] In their approach,[10] the effects of molecular weight distribution of large widths were neglected. Thus, predictions from the following equation were found to fit N_1 vs. $(\dot{\gamma}/\text{MFI})^2$ for broad and regular molecular distributions[10]:

$$N_1 = [\psi_1 \cdot (\text{MFI})^2][(\dot{\gamma}/\text{MFI})^2] \tag{1}$$

where

$$\psi_1 \cdot (\text{MFI})^2 = (\eta_0 \cdot \text{MFI})(2N/m)(\lambda \cdot \text{MFI})^2(\dot{\gamma}/\text{MFI})[1 + (\lambda \cdot \text{MFI})^2(\dot{\gamma}/\text{MFI})^2]^{-(N+1)} \tag{2}$$

N_1 is the primary normal stress difference, $\psi_1 \cdot (\text{MFI})^2$ is the modified primary normal stress function, $(\dot{\gamma}/\text{MFI})$ is the modified apparent shear rate function, $\eta_0 \cdot \text{MFI}$ is the modified zero-shear viscosity function, $\lambda \cdot \text{MFI}$ is the modified time constant, N is the parameter of the Carreau model given below, and m is the damping constant.

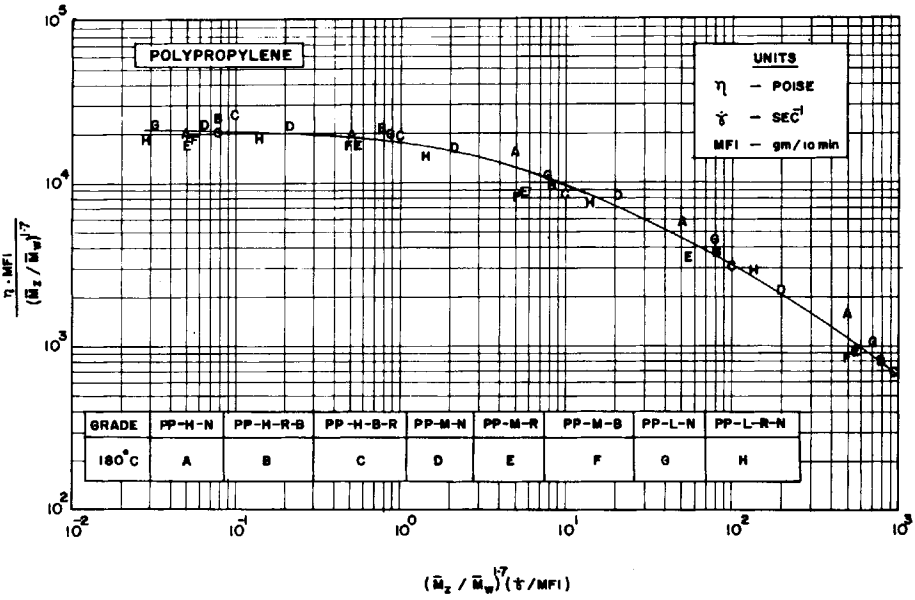

Fig. 3. Coalesced viscosity curve for broad, regular and narrow molecular weight distribution PP at 2.16-kg test load condition for MFI [(—) predictions of eq. (8)].

The derivation of eq. (2) is dependent upon the following relationships:
Modified Carreau model:

$$\eta \cdot \mathrm{MFI} = \eta \cdot \mathrm{MFI}[1 + (\lambda \cdot \mathrm{MFI})^2 \cdot (\dot{\gamma}/\mathrm{MFI})^2]^{-N} \tag{3}$$

Modified Wagner's relationship:

$$\psi_1 \cdot (\mathrm{MFI})^2 = -\frac{1}{m}\frac{d(\eta \cdot \mathrm{MFI})}{d(\dot{\gamma}/\mathrm{MFI})} \tag{4}$$

It was found by Shenoy and Saini[5] that a plot of N_1 vs. $(\dot{\gamma}/\mathrm{MFI})^2$ on a log–log scale would suffice to obtain a unified curve when the various grades of polymers

TABLE I
Molecular Characteristics of Polypropylene[a]

Grade[b]	Code	Melt flow index (190°C/2.16 kg)	$\overline{M}_w \times 10^{-5}$	$\overline{M}_z/\overline{M}_w$	$\overline{M}_z \cdot \overline{M}_w$
PP-H-N	A	4.2	2.84	2.59	20.9
PP-H-R-B	B	5.0	3.03	3.57	32.8
PP-H-B-R	C	3.7	3.39	3.54	40.7
PP-M-N	D	11.6	2.32	2.81	15.1
PP-M-R	E	12.4	2.79	4.82	37.5
PP-M-B	F	11.0	2.68	4.46	32.0
PP-L-N	G	25.0	1.79	2.47	7.9
PP-L-R-N	H	23.0	2.02	3.18	13.0

[a] From Ref. 13.

[b] H: high molecular weight; M: middle molecular weight; L: low molecular weight; N: narrow molecular weight distribution; R: regular molecular weight distribution; B: broad molecular weight distribution.

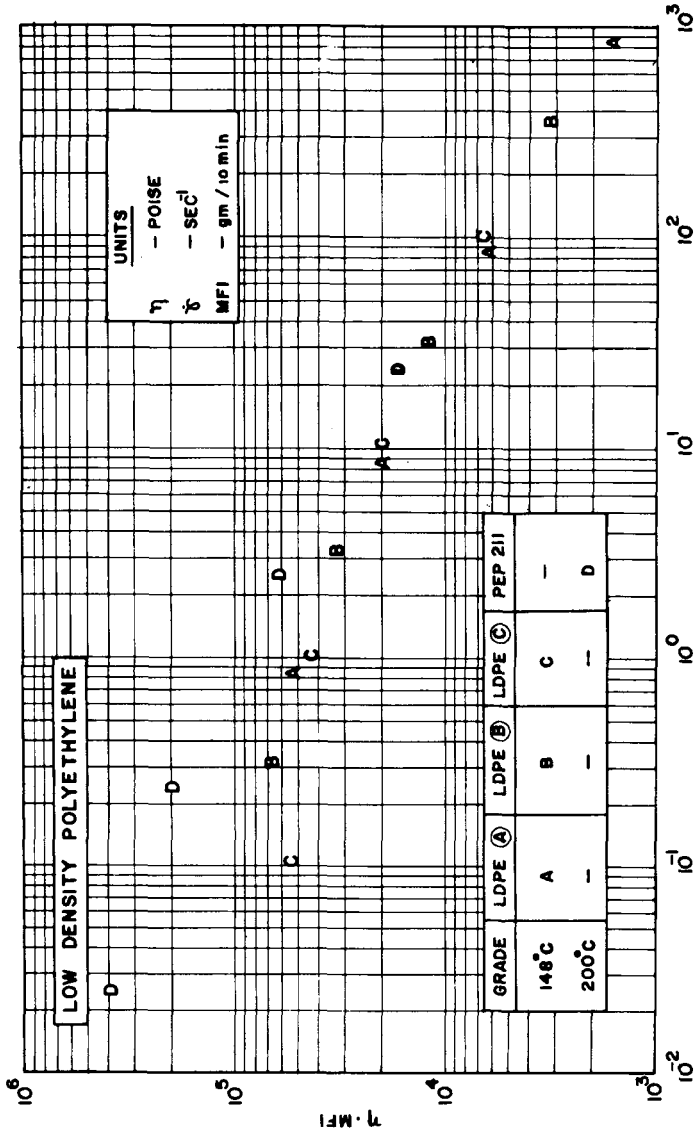

Fig. 4. Coalesced viscosity curve for LDPE at 2.16-kg test load condition for MFI.

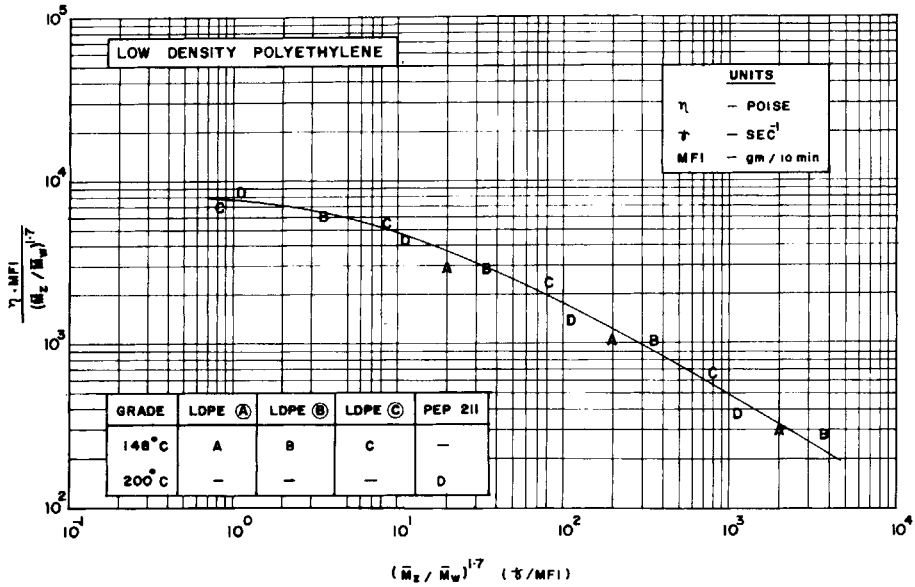

Fig. 5. Coalesced viscosity curve taking into account the molecular weight distribution for LDPE at 2.16-kg test load condition for MFI [(—) predictions of eq. (8)].

of a generic type all had broad and regular molecular weight distribution or, alternatively, all had narrow molecular weight distributions. If a unique curve is to be obtained which is independent of the width of molecular weight distribution, then a correction term $(\overline{M}_z/\overline{M}_w)^{3.5}$ is to be included so that a plot of N_1 vs. $(\overline{M}_z/\overline{M}_w)^{3.5}(\dot{\gamma}/\text{MFI})^2$ has to be used to obtain the coalescence. The following

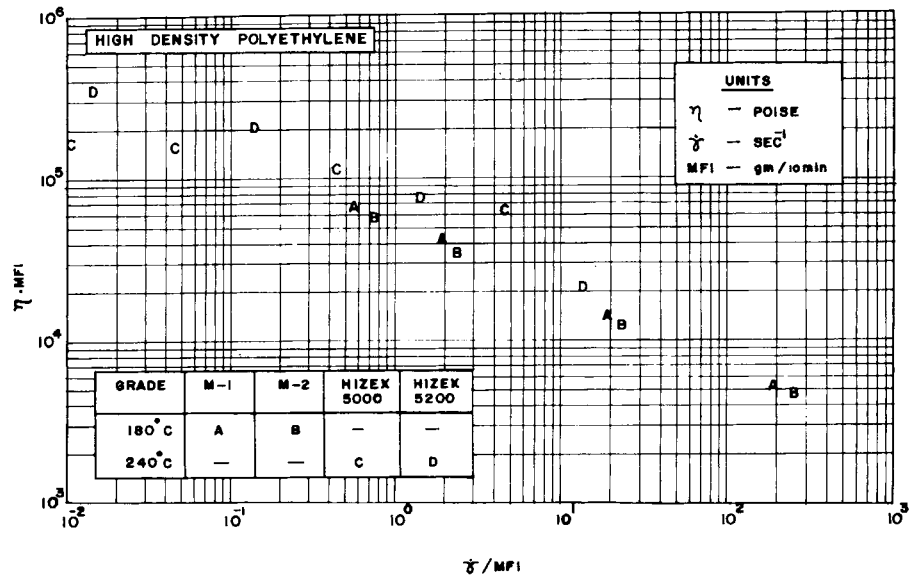

Fig. 6. Coalesced viscosity curve for HDPE at 2.16-kg test load condition for MFI.

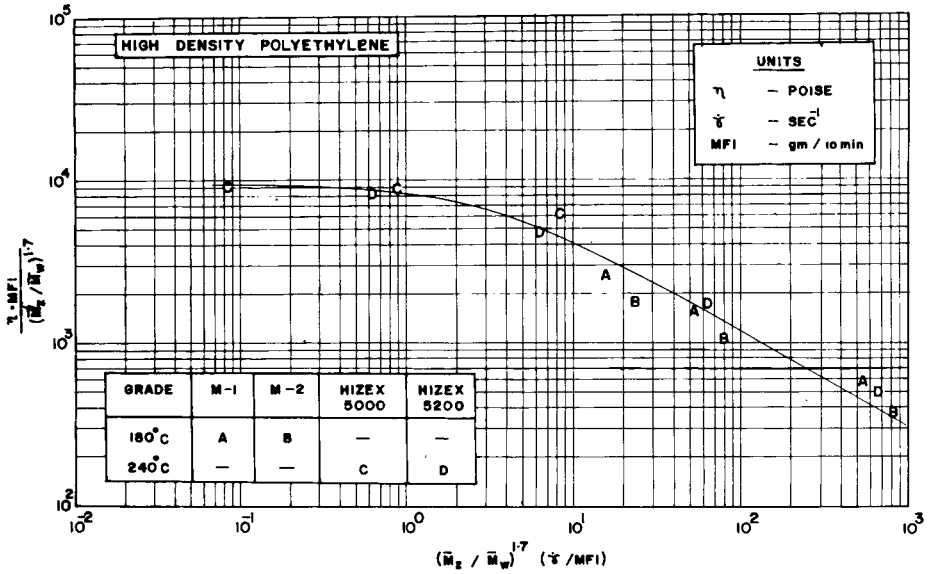

Fig. 7. Coalesced viscosity curve taking into account the molecular weight distribution for HDPE at 2.16-kg test load condition for MFI [(—) predictions of eq. (8)].

relationship between N_1, ψ_1, and $\dot{\gamma}^2$ can be written in the modified form as would fit the unique curves of Shenoy and Saini[5]:

$$N_1 = \left[\frac{\psi_1 \cdot (\mathrm{MFI})^2}{(\overline{M}_z/\overline{M}_w)^{3.5}}\right] \cdot \left[\left(\frac{\overline{M}_z}{\overline{M}_w}\right)^{3.5} \left(\frac{\dot{\gamma}}{\mathrm{MFI}}\right)^2\right] \tag{5}$$

Substituting $(\mathrm{MFI})^2/(\overline{M}_z/\overline{M}_w)^{3.5}$ for $(\mathrm{MFI})^2$ in eq. (2) gives the following:

$$\frac{\psi_1 \cdot (\mathrm{MFI})^2}{(\overline{M}_z/\overline{M}_w)^{3.5}} = \frac{(\eta_0 \cdot \mathrm{MFI})}{(\overline{M}_z/\overline{M}_w)^{1.7}} \frac{2N}{m} \frac{(\lambda \cdot \mathrm{MFI})^2}{(\overline{M}_z/\overline{M}_w)^{3.5}} \cdot \left[\left(\frac{\overline{M}_z}{\overline{M}_w}\right)^{1.7} \cdot \left(\frac{\dot{\gamma}}{\mathrm{MFI}}\right)\right] \times \left\{1 + \frac{(\lambda \cdot \mathrm{MFI})^2}{(\overline{M}_z/\overline{M}_w)^{3.5}} \left[\left(\frac{\overline{M}_z}{\overline{M}_w}\right)^{3.5} \left(\frac{\dot{\gamma}}{\mathrm{MFI}}\right)^2\right]\right\}^{-(N+1)} \tag{6}$$

Similarly, eq. (4) can be written as

$$\frac{\psi_1 \cdot (\mathrm{MFI})^2}{(\overline{M}_z/\overline{M}_w)^{3.5}} = -\frac{1}{m} \frac{d[(\eta \cdot \mathrm{MFI})/(\overline{M}_z/\overline{M}_w)^{1.7}]}{d[(\overline{M}_z/\overline{M}_w)^{1.7} \cdot (\dot{\gamma}/\mathrm{MFI})]} \tag{7}$$

Thus, combining eqs. (6) and (7) and integrating gives the following modified form of the Carreau model as

$$\frac{\eta \cdot \mathrm{MFI}}{(\overline{M}_z/\overline{M}_w)^{1.7}} = \frac{\eta_0 \cdot \mathrm{MFI}}{(\overline{M}_z/\overline{M}_w)^{1.7}} \left\{1 + \frac{(\lambda \cdot \mathrm{MFI})^2}{(\overline{M}_z/\overline{M}_w)^{3.5}} [(M_z/M_w)^{1.7} \cdot (\dot{\gamma}/\mathrm{MFI})]^2\right\}^{-N} \tag{8}$$

A plot of $(\eta \cdot \mathrm{MFI})/(\overline{M}_z/\overline{M}_w)^{1.7}$ vs. $(\overline{M}_z/\overline{M}_w)^{1.7} \cdot (\dot{\gamma}/\mathrm{MFI})$ on a log–log scale should, therefore, give a unique curve independent of the width of the molecular weight distribution, since it has been derived from the normal stress difference equation (5), which has such characteristics. It must be noted that the coalescence obtained through the correction term $(\overline{M}_z/\overline{M}_w)^{1.7}$ would not hold for higher shear rates and in the region of 10–10^3 s^{-1}, the original method of coalescence[1–4] using $\eta \cdot \mathrm{MFI}$ vs. $\dot{\gamma}/\mathrm{MFI}$ plots should work better.

TABLE II
Details of the Polymers Used in the Study

Polymers	Grade	$\overline{M}_z/\overline{M}_w$	MFI [temp (°C)/ load condition (kg)]	Data temp (°C)	No. of data points [shear rate range (s^{-1})]	Ref. no.
PP	PP-H-N	2.59	0.97[a] (180/2.16)	180	6 (0.01–400)	13
	PP-H-R-B	3.57	1.12[a] (180/2.16)	180	6 (0.01–1000)	13
	PP-H-B-R	3.54	0.85[a] (180/2.16)	180	6 (0.01–1000)	13
	PP-M-N	2.81	2.67[a] (180/2.16)	180	7 (0.13–3000)	13
	PP-M-R	4.82	2.85[a] (180/2.16)	180	4 (0.01–10)	13
	PP-M-B	4.46	2.53[a] (180/2.16)	180	6 (0.01–1000)	13
	PP-L-N	2.47	5.75[a] (180/2.16)	180	7 (0.01–7500)	13
	PP-L-R-N	3.18	5.29[a] (180/2.16)	180	7 (0.02–6500)	13
LDPE	A	6.63	0.12[b] (148/2.16)	148	4 (0.1–100)	14
	B	4.12	0.32[b] (148/2.16)	148	4 (0.1–100)	14
	C	3.37	0.94[b] (148/2.16)	148	4 (0.1–100)	14
	PEP 211	9.46	4.10[b] (200/2.16)	200	4 (0.1–100)	15
HDPE	M-1	6.90	0.51[b] (180/2.16)	180	4 (0.3–100)	16
	M-2	7.78	0.42[b] (180/2.16)	180	4 (0.3–100)	16
	HIZEX 5000	5.60	2.16[b] (240/2.16)	240	4 (0.01–10)	17
	HIZEX 5200	9.30	0.70[b] (240/2.16)	240	4 (0.01–10)	17

[a] MFI values calculated through WLF-type equation in Ref. 1, knowing the MFI values under standard conditions as given in Table I.
[b] MFI values calculated from the shear stress vs. shear rate curves in accordance with the read out method used in Ref. 4.

TABLE III
Rheological Parameters of the Modified Carreau Model [Eq. (8)] for Polyolefins Considered in the Study

Polymer type	$\frac{\eta_0 \cdot \text{MFI}}{(\overline{M}_z/\overline{M}_w)^{1.7}}$	$\frac{\lambda \cdot \text{MFI}}{(\overline{M}_z/\overline{M}_w)^{1.7}}$	N	Applicability range of $(\overline{M}_z/\overline{M}_w)^{1.7} \cdot (\dot{\gamma}/\text{MFI})$
Polypropylenes	2.2×10^4	1.0	0.22	0.1–1000
Low density polyethylenes	8.0×10^3	0.31	0.25	1–1000
High density polyethylenes	9.5×10^3	0.50	0.26	0.1–1000

RESULTS AND DISCUSSION

Figures 1 and 3 show plots of η·MFI vs. $\dot{\gamma}$/MFI in log–log scales for a number of polymer grades of polypropylene described in Table I. The eight different polymer samples have been found to give two distinct unified curves in the low shear rate region coalesing the data for four grades each. Molecular characteristics of the samples show that B, C, E, and F form a distinct group with broad and regular molecular weight distribution while A, D, G, and H form another group with narrow molecular weight distribution. In the low shear rate region of 10^{-2}–10 s^{-1}, Figures 1 and 2 do not superimpose as they stand. However, in accordance with the analysis provided earlier, a plot of $(\eta\text{·MFI})/(\overline{M}_z/\overline{M}_w)^{1.7}$ vs. $(\overline{M}_z/\overline{M}_w)^{1.7}$ $(\dot{\gamma}/\text{MFI})$ should yield a unique curve taking care of the differences in the width of the molecular weight distribution. Figure 3 shows such a plot. The values of $(M_z/M_w)^{1.7}$ alone do not control the coalescence as it is clear that the normalizing factor for unifying the viscosity vs. the shear rate curves of widely different molecular weight distribution is more truly $(\overline{M}_z/\overline{M}_w)^{1.7}/\text{MFI}$. Now it is known that η varies directly as $\overline{M}_w^a$, where a takes the value of about 3.4 for

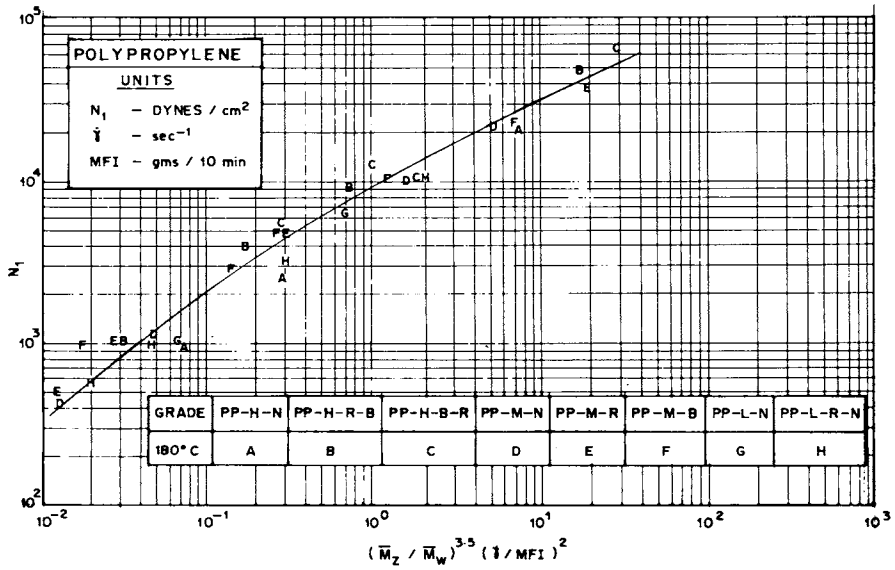

Fig. 8. Coalesced normal stress difference curve for broad, regular, and narrow molecular weight distribution PP at 2.16-kg test load condition for MFI [(—) shows the predictions of eq. (6)].

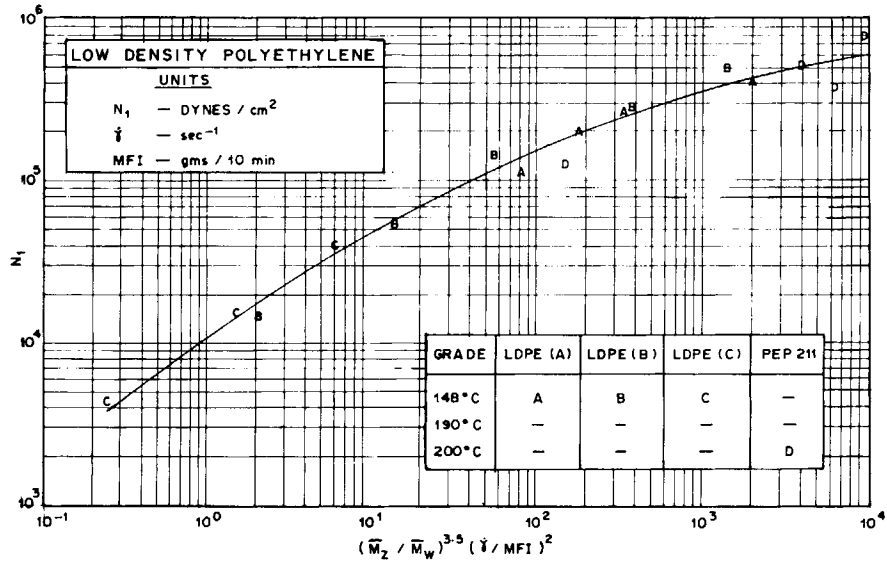

Fig. 9. Coalesced normal stress difference curve taking into account the molecular weight distribution for LDPE at 2.16-kg test load condition for MFI [(—) predictions of eq. (6)].

zero-shear viscosity and decreases slightly for viscosities at higher shear rates. Shenoy et al.[1–4] have shown that MFI varies inversely as viscosity, and hence it can be assumed that MFI would vary inversely as $\overline{M}_w^{3.4}$ as a first approximation. This suggests that the normalizing factor is controlled in the correct sense by the value of $(\overline{M}_z \cdot \overline{M}_w)^{1.7}$. Hence, all the grades of a particular generic type of polymer which have values of $\overline{M}_z \cdot \overline{M}_w$ nearer to each other would be expected to coalesce. The values of $(\overline{M}_z \cdot \overline{M}_w)$ for the eight grades of polypropylene are

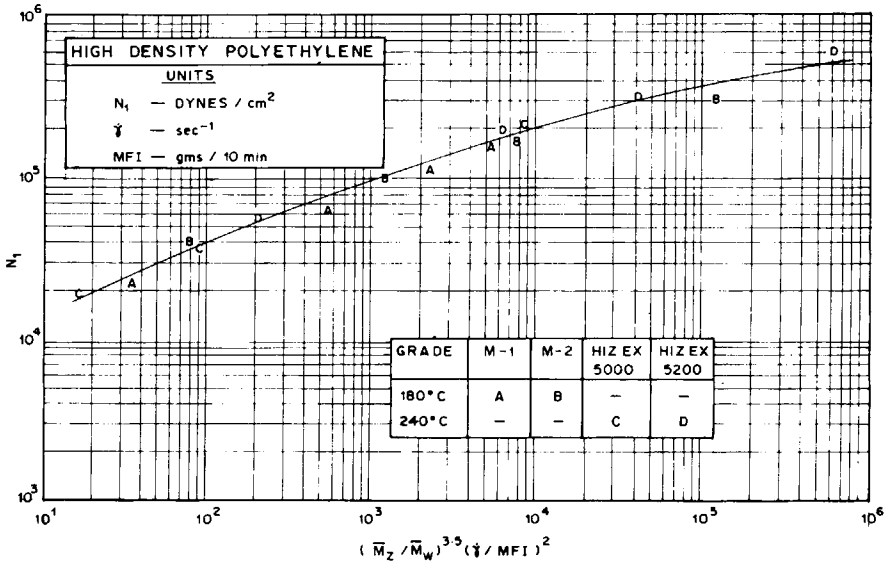

Fig. 10. Coalesced normal stress difference curve taking into account the molecular weight distribution for HDPE at 2.16-kg test load condition for MFI [(—) predictions of eq. (6)].

TABLE IV
Material Parameter of Eq. (6) for Different Polyolefins Considered in the Study

Polymer type	Damping constant m
Polypropylenes	0.4
Low density polyethylenes	0.1
High density polyethylenes	0.3

given in Table I, and it is then clear why B, C, E, and F form a distinct group while A, D, G, and H form another distinct group for the coalescence. This would explain why even two grades with similar $(\overline{M}_z/\overline{M}_w)$ but different $\overline{M}_w$ characteristics and consequently different rheological characteristics would have a coalesced curve because the sensitive parameter for unification is not $(\overline{M}_z/\overline{M}_w)$ but $\overline{M}_z \cdot \overline{M}_w$. In cases where $(\overline{M}_z/\overline{M}_w)$ is the same, the viscosity vs. shear rate curves would coalesce simply through MFI as the normalizing factor as it would account for all changes in $\overline{M}_w$. Figure 4 shows a plot of η·MFI vs. $\dot{\gamma}$/MFI for four different low density polyethylene melts. In the low shear rate region of 10^{-2}–10 s^{-1}, the coalescence is rather poor. A plot of $(\eta \cdot \text{MFI})/(\overline{M}_z/\overline{M}_w)^{1.7}$ vs. $(\overline{M}_z/\overline{M}_w)^{1.7}$ $(\dot{\gamma}/\text{MFI})$ for the same four low density polyethylene melts was found to give a unified curve as shown in Figure 5. Figures 6 and 7 show the similar effects produced by the correction term of $(\overline{M}_z/\overline{M}_w)^{1.7}$ on the high density polyethylene low shear data. Figures 3, 5, and 7 thus show plots which are independent of grade, temperature, and molecular weight distribution in the low shear rate region. Molecular weight distribution is often expressed as one of the following ratios, namely, $\overline{M}_w/\overline{M}_n$, $\overline{M}_z/\overline{M}_w$, $\overline{M}_{z+1}/\overline{M}_z$, etc. An approximate interrelationship between the various expressions has been given by Van Krevelan et al.[12] based on the analysis of data for a number of polymers:

$$\overline{M}_w/\overline{M}_n = Q, \qquad \overline{M}_z/\overline{M}_w \approx Q^{0.75}, \quad \frac{\overline{M}_z}{\overline{M}_n} \approx Q^{1.75}$$

$$\overline{M}_{z+1}/\overline{M}_z \approx Q^{0.56}, \quad \overline{M}_{z+1}/\overline{M}_n \approx Q^{2.31} \tag{9}$$

$$\overline{M}_z\overline{M}_{z+1}/\overline{M}_w^2 \approx Q^{2.06}, \quad \frac{\overline{M}_z\overline{M}_{z+1}}{\overline{M}_n^2} \approx Q^{4.06}$$

Any of the above expressions could thus be used in place of $(\overline{M}_z/\overline{M}_w)^{1.7}$ in the unified curve through proper conversion. The details of all the polymers used for getting Figures 1–7 have been given in Table II.

The plots shown in Figures 3, 5, and 7 can be readily fitted by the modified Carreau model as given by eq. (8) as the data covered all falls within the low shear rate range of validity of the model. The solid line in each of the curves shows the fit. The parameters of the model are given in Table III for each generic type of

TABLE V
Value of n To Be Used in Eq. (10) for the Polyolefins Considered in the Study

Polymer type	n
Polypropylenes	0.34
Low density polyethylenes	0.46
High density polyethylenes	0.54

TABLE VI
Flow Activation Energies for the Polyolefins Considered in the Study[18]

Polymer type	E (kcal/mol)	Temperature range of validity (°C)
Polypropylenes	9.87	200–250
Low density polyethylenes	7.25	175–205
High density polyethylenes	6.83	175–220

polymer. Since eq. (8) is derived from eq. (6), a natural fit of eq. (6) to the unified normal stress difference curves of N_1 vs. $(\overline{M}_z/\overline{M}_w)^{3.5}\cdot(\dot{\gamma}/\text{MFI})^2$ given by Shenoy and Saini[5] can be expected. Figures 8–10 are reproduced from Shenoy and Saini[5] along with the solid line which shows the fit of eq. (6) to the curve. The dampening constant m required for the curve modeling has been given in Table IV.

The unified viscosity curves in Figures 3, 5, and 7 along with the unified normal stress difference curves in Figures 8, 9, and 10 form a set from which the viscoelastic property of a polyolefin melt can be estimated in the low shear rate region merely from the knowledge of its MFI.

The steps involved in generating the viscosity and normal stress difference curves at the temperature of interest are as follows:

—The MFI value has to be obtained under standard temperature and load test conditions either from the polymer manufacturer or as determined through a measurement on the melt flow apparatus.

—The loading condition of the obtained MFI must be the same as that specified in the unified curve. If it is different, a new value of MFI ought to be calculated[1] using the following equation:

$$\text{MFI}(L_2)/\text{MFI}(L_1) = (L_2/L_1)^{1/n} \tag{10}$$

where L_1 and L_2 are the test load and the load at which MFI is required, respectively. The values of n to be used for the different polyolefins are given in Table V.

—The temperature of MFI measurement should be checked with the temperature at which the viscosity and the elasticity curve is desired. Using one of the two following equations, the MFI at the required temperature should be calculated:

Modified WLF-type equation[1]:

$$\log\frac{\text{MFI}(T_2)}{\text{MFI}(T_1)} = \frac{8.86\,(T_2 - T_s)}{101.6 + (T_2 - T_s)} - \frac{8.86\,(T_1 - T_s)}{101.6 + (T_1 - T_s)} \tag{11}$$

Modified Arrhenius type equation[18]:

$$\frac{\text{MFI}(T_2)}{\text{MFI}(T_1)} = \exp\left[\frac{E}{R}\left(\frac{1}{T_1} - \frac{1}{T_2}\right)\right] \tag{12}$$

where T_1 is the ASTM-recommended test temperature (°K), T_2 is the temperature at which MFI is required (°K), T_s is the standard reference temperature ($= T_g + 50$) (°K), T_g is the glass transition temperature of the polymer (°K), R is the gas constant, and E is the activation energy for viscous flow as tabulated in Table VI for the three types of polyolefins.

The choice of eqs. (11) or (12) to determine the temperature dependence of MFI is mainly governed by whether $T < T_g + 100$ or $T > T_g + 100$. At tem-

peratures relatively nearer to T_g, free volume and its changes with temperature play a dominant role. Hence the modified WFL-type equation (11) would provide better estimates. At temperatures greater than $T_g + 100$, the temperature dependency of MFI is decisively affected by overcoming of the forces of intermolecular interactions. Hence the modified Arrhenius type equation (12) would give better predictions in such cases.

—The molecular weight distribution should be known either through the manufacturer's grade specifications or through conventional measurement. The MWD value should be obtained in terms of $\overline{M}_z/\overline{M}_w$. If obtained in any other form like $\overline{M}_w/\overline{M}_n$ or $\overline{M}_z\overline{M}_{z+1}/\overline{M}_w$, then it should be converted to $\overline{M}_z/\overline{M}_w$ using eq. (9).

—The plots of η vs. $\dot{\gamma}$ and N_1 vs. $\dot{\gamma}^2$ under the required conditions can be readily obtained by substituting the correct value of MFI and $\overline{M}_z/\overline{M}_w$ in the appropriate unified curve.

CONCLUSIONS

The inherent limitation existing in the unified curves presented by the authors[1–4] has been overcome by using a correction term of $(\overline{M}_z/\overline{M}_w)^{1.7}$ in order to account for molecular weight distribution during the coalescence of the viscosity curves. The unified curves presented herein are not only grade- and temperature-invariant but are also independent of the width of molecular weight distribution in the lower shear rate region, where such effects of MWD are seen. When using these unified curves, care must be taken to restrict their use only to low shear rate region (10^{-2}–$10\ s^{-1}$) as the correction term of $(\overline{M}_z/\overline{M}_w)^{1.7}$ would not be effective for coalescence in the higher shear rate regions of 10–$10^3\ s^{-1}$. In such high shear rate regions, the original coalesced curves of the authors[1–4] would be most suitable.

References

1. A. V. Shenoy, S. Chattopadhyay, and V. M. Nadkarni, *Rheol. Acta*, **22,** 90 (1983).
2. A. V. Shenoy, D. R. Saini, and V. M. Nadkarni, *J. Appl. Polym. Sci.*, **27,** 4399 (1982).
3. A. V. Shenoy, D. R. Saini, and V. M. Nadkarni, *J. Vinyl Tech.*, **5,** 192 (1983).
4. A. V. Shenoy, D. R. Saini, and V. M. Nadkarni, *Rheol. Acta*, **22,** 209 (1983).
5. A. V. Shenoy and D. R. Saini, *Rheol. Acta*, to appear.
6. D. J. Smith, *Tappi*, **60,** 131 (1977).
7. F. J. Borzenski, *Plastics Compounding*, (Sept/Oct), 25 (1978).
8. M. Shida and L. V. Cancio, *Polym. Eng. Sci.*, **11,** 124 (1971).
9. K. Oda, J. L. White, and E. S. Clark, *Polym. Eng. Sci.*, **18,** 25 (1978).
10. A. V. Shenoy and D. R. Saini, *Chem. Eng. Commun.*, to appear.
11. W. H. Wagner, *Rheol. Acta*, **16,** 43 (1977).
12. D. W. Van Krevelan, D. J. Goedhar, and P. J. Hoftijzer, *Polymer*, **18,** 750 (1977).
13. W. Minoshima, J. L. White, and J. E. Spruiell, *Polym. Eng. Sci.*, **20,** 1166 (1980).
14. A. Ram, *Polym. Eng. Sci.*, **17,** 793 (1977).
15. C. D. Han, K. U. Kim, N. Siskovic, and C. R. Huang, *Rheol. Acta*, **14,** 533 (1975).
16. C. W. Macosko and J. M. Lornstson, Soc. Plast. Eng. of ANIEC, Tech. Pap., **19,** 461 (1973).
17. C. D. Han and S. M. Apte, *J. Appl. Polym. Sci.*, **24,** 61 (1979).
18. D. R. Saini and A. V. Shenoy, *J. Macromol. Sci. Phys.*, **B22,** 437 (1983).

Received June 13, 1983
Accepted November 11, 1983